Focal ratio degradation and transmission in VIRUS-P optical fibers

Murphy, Jeremy, MacQueen, Phillip, Hill, Gary, Grupp, Frank, Kelz, Andreas, et al.

Jeremy D. Murphy, Phillip J. MacQueen, Gary J. Hill, Frank Grupp, Andreas Kelz, Povilas Palunas, Martin Roth, Alexander Fry, "Focal ratio degradation and transmission in VIRUS-P optical fibers," Proc. SPIE 7018, Advanced Optical and Mechanical Technologies in Telescopes and Instrumentation, 70182T (23 July 2008); doi: 10.1117/12.788411

SPIE.

Event: SPIE Astronomical Telescopes + Instrumentation, 2008, Marseille, France

Focal Ratio Degradation and Transmission in VIRUS-P Optical Fibers

Jeremy D. Murphy[a], Phillip J. MacQueen[b], Gary J. Hill[b],
Frank Grupp[c], Andreas Kelz[d], Povilas Palunas[b,e],
Martin Roth[c], Alexander Fry[a]

[a]The University of Texas, Department of Astronomy
1 University Station C1400, Austin, Texas, USA 78712-0259
[b]The University of Texas, McDonald Observatory
1 University Station C1402, Austin, Texas, USA 78712-0259
[c]Universitäts-Sternwarte, München, Germany
Scheinerstr. 1, D-81679 München, Germany
[d]Astrophysikalisches Institut Potsdam
An der Sternwarte 16, 14482 Potsdam, Germany
[e]Las Campanas Observatory, Chile
Colina El Pino, La Serena, Chile

ABSTRACT

We have conducted extensive tests of both transmission and focal ratio degradation (FRD) on two integral field units currently in use on the VIRUS-P integral field spectrograph. VIRUS-P is a prototype for the VIRUS instrument proposed for the Hobby-Eberly Telescope at McDonald Observatory. All tests have been conducted at an input f-ratio of F/3.65 and with an 18% central obscuration in order to simulate optical conditions on the HET. Transmission measurements were conducted with narrow-band interference filters (FWHM: 10 nm) at 10 discrete wavelengths (337 to 600 nm), while FRD tests were made at 365 nm, 400 nm and 600 nm. The influence of wavelength, end immersion, fiber type and length on both FRD and transmission is explored. Most notably, we find no wavelength dependence on FRD down to 365 nm. All fibers tested are within the VIRUS instrument specifications for both FRD and transmission. We present the details of our differential FRD testing method and explain a simple and robust technique of aligning the test bench and optical fiber axes to within ±0.1 degrees.

Keywords: Optical Fibers, Focal Ratio Degradation, VIRUS-P, HETDEX

1. INTRODUCTION

The versatility provided by optical fibers in the design of astronomical instrumentation is making their use commonplace. Fiber-fed spectrographs are being used widely and with great success.[1–3] As the demand for fiber-fed instrumentation increases, so does the need for a clear understanding of the two dominant processes that dictate fiber quality and applicability, namely transmission and focal ratio degradation (FRD). Relatively simple and accurate methods to test fiber transmission have been in use for many years, yielding results that prove very repeatable from group to group.[4–6] However, accurate FRD measurements have proven more challenging, in large part due to two causes: 1) The measurement techniques and instruments available have often lacked the precision to measure the faint halos associated with FRD, particularly at relatively fast input beams where FRD is expected to be small, and 2) The variety of sources of FRD are often intertwined, so that repeatability of the results from group to group has been elusive.

Despite these challenges, many groups have made accurate FRD measurements and our understanding of FRD continues to improve[7–11] We now know FRD exhibits a strong dependence on the quality of end polish

Send correspondence to: murphy@astro.as.utexas.edu

Advanced Optical and Mechanical Technologies in Telescopes and Instrumentation, edited by Eli Atad-Ettedgui, Dietrich Lemke, Proc. of SPIE Vol. 7018, 70182T, (2008) · 0277-786X/08/$18 · doi: 10.1117/12.788411

and immersion, bending and radial stresses due to fiber handling and mounting methods. FRD also exhibits a weaker dependence on length and fiber type. Its dependence on wavelength has been studied by Ramsey ('88) Avila ('88) and Schmoll ('03) among others, where they found little to no wavelength dependence. However, the majority of wavelength-dependent FRD tests have been conducted through broadband filters,[4] were not conducted on a statistical number of fibers, or did not test wavelengths below 400 nm. Our tests, particularly at near-UV wavelengths, are motivated by the VIRUS 350 nm blue limit and this lack of data in the literature.

We have undertaken transmission and FRD measurements of two integral field units (IFU) currently in use on the VIRUS-P integral field spectrograph.[12] VIRUS-P has been in use on the 2.7m Harlan J. Smith telescope at McDonald Observatory since Fall, 2006. It is a prototype for the VIRUS instrument proposed for the Hobby-Eberly Telescope Dark Energy eXperiment (HETDEX). HETDEX is a spectroscopic survey with the goal of collecting spectra of nearly one million Lyman-alpha emitting galaxies between a redshift of 1.8 to 3.5 in order to place constraints on dark energy.[13] VIRUS will be composed of approximately 150 spectrographs, each fed by an IFU. The science requirements of the HETDEX project is weighted towards optimal transmission in the blue. In order to gain a comprehensive understanding of both transmission and FRD over the entire wavelength range of the VIRUS spectrograph (340 nm to 540 nm) a fiber optic test bench has been constructed at the University of Texas, Austin.

The paper outline is as follows. In section 2 we briefly describe the results of tests conducted at the University Observatory, Munich, on the effects of length, bending, end immersion, fiber type and input f-ratio on FRD. Details of the fabrication of both IFUs is given in section 2.1. This is relevant as we find FRD in the shorter IFU (VP1) to be worse than the longer bundle (VP2) and is likely a result of the different fabrication techniques employed. In section 3 we give details of the test bench constructed at the University of Texas, Austin. Section 4 discusses the testing method used for both FRD and transmission measurements. Sections 5 and 6 summarize the primary results of our FRD and transmission tests respectively.

2. PRELIMINARY TESTS

The Photometric Test Bench[14] at the Astrophysical Institut Potsdam (AIP) was used to conduct a variety of FRD measurements on different fiber types and numerical aperture (NA).[15] The influence of bending, fiber length and immersion on FRD was also explored. Many of these results guided aspects of the design for the VIRUS-P spectrograph and the two prototype IFUs. We include here two figures showing FRD dependence as a function of input f-ratio on fiber length and end immersion. Fiber immersion involved contacting the input end of the fiber to an anti-reflective (AR) cover plate. The fiber-glass interface was made with an index matching gel. The significant results of tests conducted at AIP are as follows: The output f-ratio for an input of F/3.65 showed little to no appreciable FRD over the majority of tests conducted. These included tests on fiber type and core diameter,* bending tests down to a radius of 10 mm, length and fiber NA.† However, at input beams slower than F/4, FRD was seen to increase with all the tests mentioned above. This was most predominant in the bend tests; at an input of F/4, no appreciable difference in an FRD value of 1.11‡ was seen over the bend radii explored (250 to 10 mm). At an input of F/6, FRD increased from 1.13 to 1.5 over the same bend radii, and by an input of F/10 an increase in FRD from 1.25 to 2.32 was observed.

In sharp contrast to these results (where FRD is small for an input f-ratio of F/3.65) is the significant effect fiber end immersion has in improving FRD at all but the fastest input beams. This is not surprising, as fiber end effects have been shown by many groups to dominate over all other sources of FRD. The notable exception to this is extreme cases of radial pressure and micro bends.

The VIRUS-P spectrograph is designed to accept an F/3.36 input beam in order to meet the science requirement of 95% encircled energy (EE) within F/3.65. The remainder of the results presented in this paper were conducted at the fixed input of F/3.65. We find that all fibers tested are performing within this specification for FRD, with ∼50% reaching 99% EE at the F/3.36 limit. The details of these results are found in section 5.

*Four Polymicro fibers were tested: FBP200, FLP200, FLP150 and FVP100.

†Fibertech AS200 NA:0.16, AS200 NA:0.22 and Polymicro FBP200 NA:0.22.

‡Here, and for the remainder of this paper, we define FRD as the ratio of the output f-ratio (95% encircled energy) to the input f-ratio; no FRD has a value of 1. The FRD value of 1.11 is likely inflated due to issues with coupling misalignment.

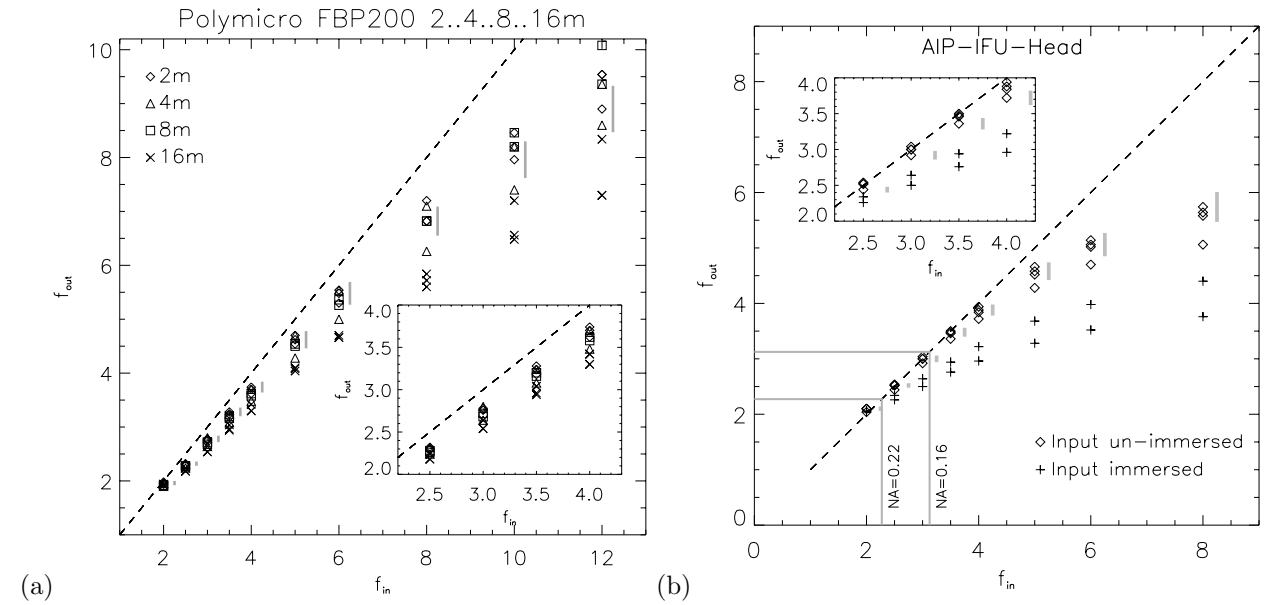

Figure 1. Figure (a) plots output f-ratio vs. input f-ratio for 4 different fiber lengths (Polymicro FBP200/220/245). The multiple measurements shown come from testing the same length of fiber from opposite ends. Although FRD increases with the input f-ratio, it is unclear whether this is due strictly to increasing fiber length. Note that while the 16 m length exhibits the worst FRD, both the 2 m and 4 m lengths show higher FRD than the 8 m length. In either case, the FRD at our input f-ratio of F/3.65 is minimal. Figure (b) shows the results of end immersion on the VIRUS-P IFU, VP1. The diamonds show results from end immersion while the plus symbols are bare fiber measurements. The benefit of immersion at all input f-ratios is clear.

2.1 Integral Field Unit Fabrication

Two different IFUs were fabricated for use on the VIRUS-P instrument. The first, VP1, was fabricated at AIP with 247 Polymicro 200 μm fibers (FBP200/220/245) to a length of 4.5m.[16] In order to explore transmission and FRD properties of a variety of fibers, 4 different fiber types[§] were used to fabricate the second IFU, VP2. Constructed by Frank Optic, VP2 is 15 m long allowing VIRUS-P to be tested on the HET.

For both VP1 and VP2 the input end of the IFU was fabricated by inserting the individual fibers into silica capillary tubes to ensure accurate alignment and uniform spacing. The output end of the two IFUs was mounted in the same configuration, but fabricated and polished differently. For VP1, each fiber was polished individually before being mounted into the output slit arrangement. In VP2, the fibers were mounted and fixed into their final alignment *before* polishing. The ends of all fibers were then polished simultaneously. This difference in the mounting and polishing method is likely the reason why VP1 exhibits worse FRD than VP2, despite the length difference (figure 9).

3. THE FIBER OPTIC TEST BENCH

To conduct FRD and transmission tests over the wavelength range of VIRUS-P, a new test bench was constructed at the University of Texas, Austin. To avoid the difficulties due to chromatic aberration inherent to lens-based optical systems, particularly below 400 nm, our test bench employs mirrors to collimate the light and re-image the input pinhole onto the fiber. A schematic of the test bench is given in figure 3. Numbers in parentheses following the description given below refer to the optical elements as referenced in the figure.

The light source is from Oriel and uses a low-ozone deuterium OSRAM XBO bulb (1). To remove the strong non-uniformities of the source profile shape, the light passes through two fused silica lambertian diffusers (2).

[§]The 4 fiber types used in VP2 are: Polymicro FBP200/220/245, NA:0.22, Fibertech As200/220UVPI, NA:0.22 and 0.16, and CeramOptec UV200/220P, NA:0.22.

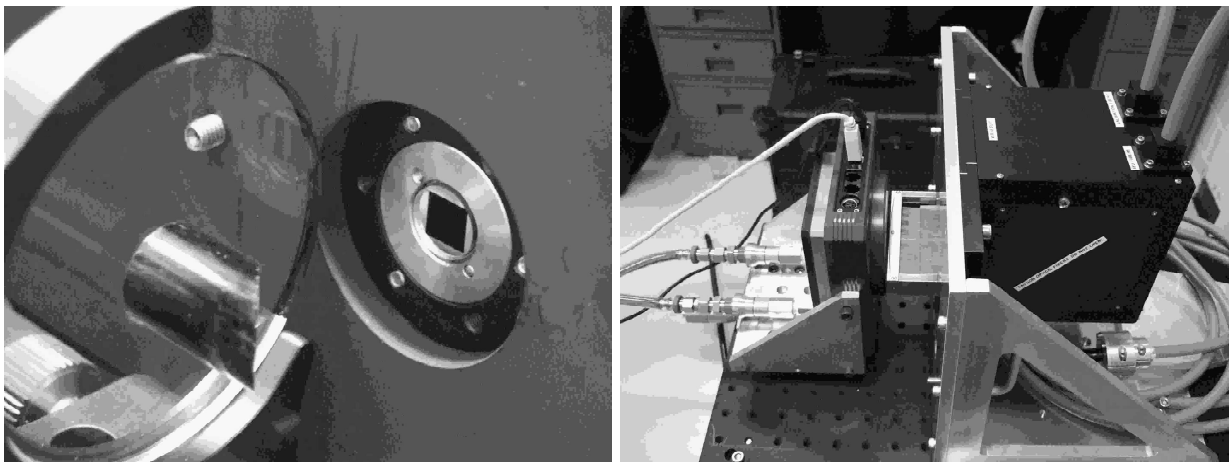

Figure 2. The left picture shows the IFU head mounted to its XYZ translation stage. Only the fiber input end (black square) is visible. For reference, this square is ∼5 mm across. The second cylindrical pickoff mirror is seen to the left. The right image shows the output slit of the IFU mounted for testing. The CCD camera, mounted on its translation stage, is seen on the left.

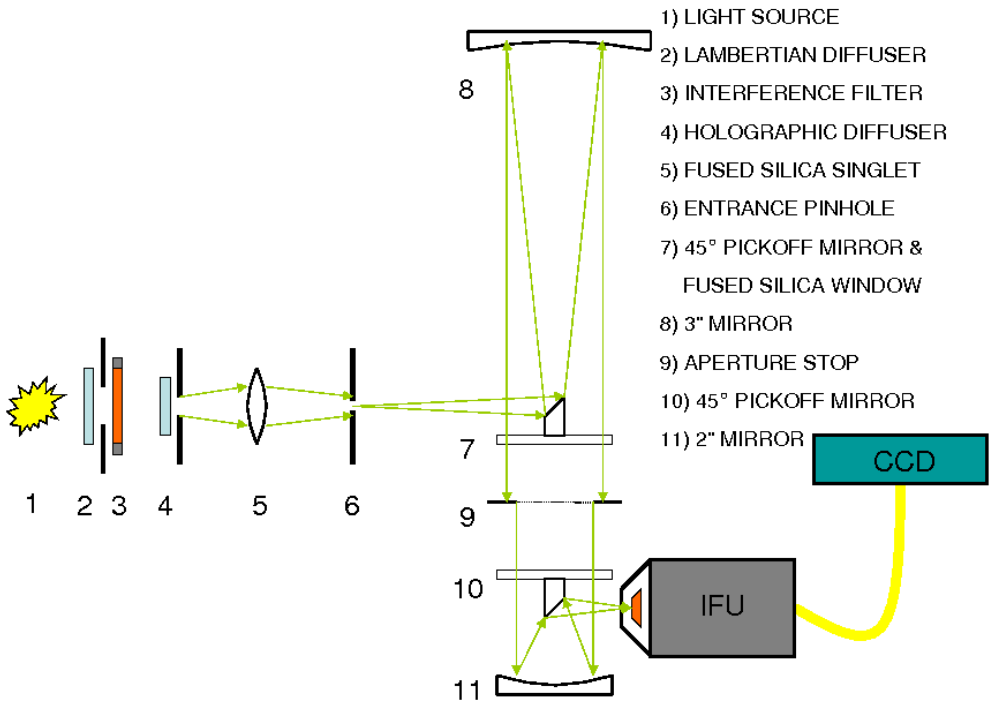

Figure 3. A schematic of the test bench. The use of mirrors over achromat lenses allows us to test over our entire wavelength range of 337 nm to 600 nm without refocusing. The image quality of the system is good at all wavelengths as evidenced by the sharp input spots at all wavelengths (figure 5).

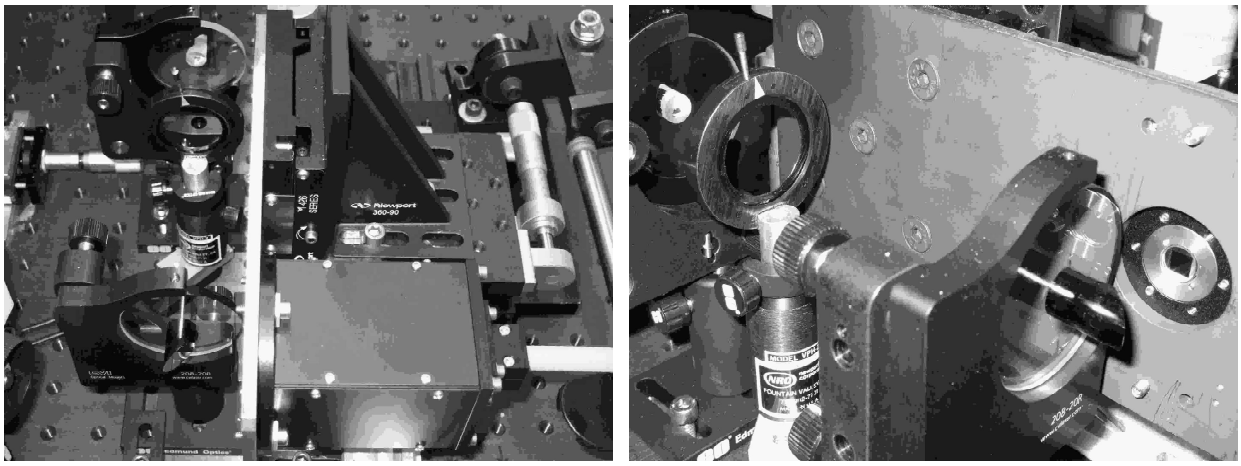

Figure 4. Two images of the test bench. In the foreground of the first image the IFU input head is shown mounted to its XYZ translation stage. On the left side of this image one sees both pickoff mirrors and the aperture stop of the system (elements 7, 9 and 10 in figure 3). The second mirror (11) is just out of the frame. The right image shows another view of the aperture stop, second pickoff mirror and IFU head mounting stage.

After an irising baffle, the filters follow (3).¶ The light is filtered with a set of 10 narrow-band (FWHM: 10 nm) interference filters (CVI Laser) with central wavelengths of 337, 350, 365, 380, 400, 420, 450, 500, 550 and 600 nm. A 10 degree forward scattering holographic diffuser (4) follows the filter and then a second baffle. The light is then focused onto the entrance pinhole (6) with a fused silica singlet (5). The pinhole is interchangeable with two different sizes used for either FRD or transmission measurements. The magnification of the system, set by the two collimating mirrors, is 0.23. Thus, a 400 μm pinhole images to 96 μm at the test bench focus and is used for all transmission measurements. For our FRD measurements a 1000 μm pinhole is used. This size pinhole images to 230 μm and assures complete illumination over the face of the 200 μm fibers tested.

After the light exits the pinhole, it is caught by the first of two cylindrical 45-degree pickoff mirrors (7) mounted to a fused silica window and sent to the first mirror (D:76.2 mm f:406.4 mm) (8). Collimation of the system is made by adjusting the position of the entrance pinhole, which is slaved to the lens. The collimated beam then passes back to the first window where the pick-off mirror (10 mm in diameter) mimics the central obscuration of the Hobby-Eberly Telescope (HET). As the VIRUS-P instrument employs a Schmidt camera, we are interested in the FRD effects that send light into the central obscuration as well as out of the entrance cone angle. After the beam passes through this window the aperture stop of the test bench is set with an adjustable iris (9), and dictates the input f-ratio of the system. The beam then passes through another fused silica window and is focused onto the second pickoff mirror by another mirror (D: 50.8 mm, f:101.6 mm) (11). The light is then sent to focus onto either the IFU, which is mounted to an XYZ translation stage, or to the CCD camera. Coupling into the fibers is done visually and aided by a microscope. An image of both the pickoff mirrors and the iris aperture is shown in figure 4. The input end of the IFU, attached to its translation stage, is seen just to the right of the second pickoff mirror in the left-hand image. The image quality of our test bench is good, delivering uniform and sharp images of the pinhole and central obscuration. Figure 5 shows typical images of both the input and output spot.

3.1 Alignment and Coupling Efficiency

Any non-orthogonality at the input end of the fiber between the optical and fiber axes introduces artificial FRD. Therefore alignment of the translation stage and IFU head to the optical axis of the test bench is critical. The

¶Although placement of the interference filters in uncollimated light introduces a slight wavelength shift from the filter's central wavelength this choice was necessary; each filter is slightly wedge shaped, leading to shifts in the position of the output spot when the filter is placed in the collimated beam. Although the shifts are small (30 to 100 μm) this is enough to make efficient and repeatable coupling into the fibers very difficult, necessitating this move.

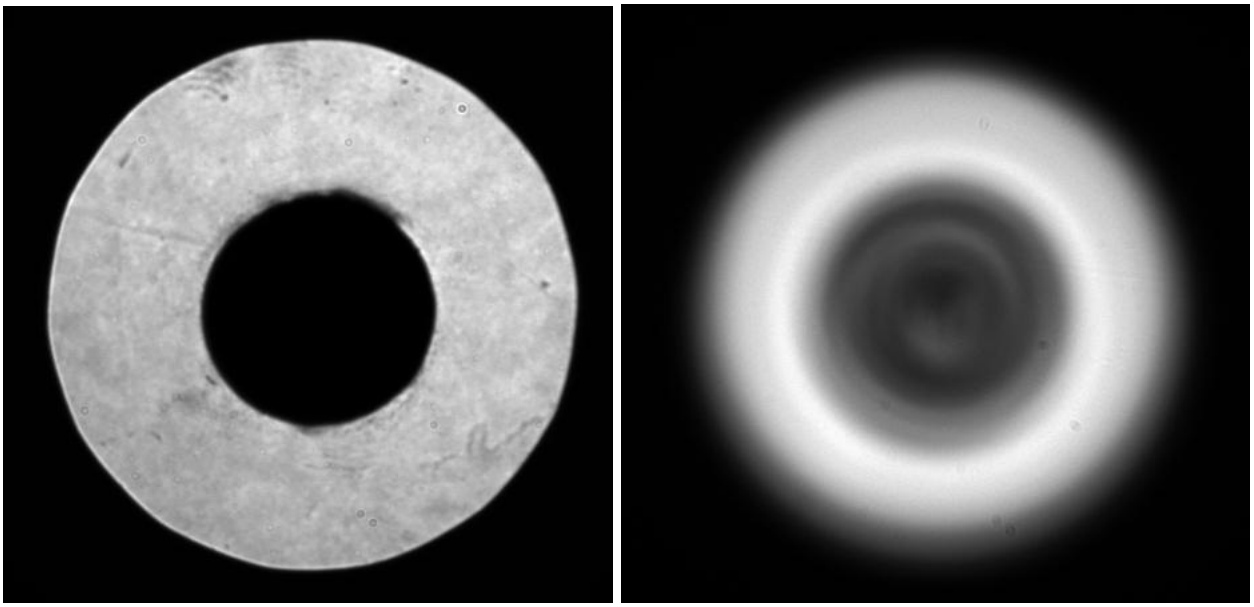

Figure 5. Far field images of the input and output spots taken with the 400 μm pinhole. The central obscuration, defined by the pickoff mirrors, is very sharp in the input spot, with its peak-to-valley edge transition happening over a few pixels. A typical output spot is seen to the right where FRD has scattered light both outwards and into the central obscuration.

initial alignment of the test bench was done by feeding a laser back through the system and aligning the return beam with the input beam. This allows us to determine orthogonality of the input beam to the IFU mounting plate to within ± 0.01 radians. This, however, is not good enough. According to equation 1, taken from Avila (1988), a 0.01 radian error in the input angle, θ, at an input f-ratio of F/3.65, will introduce $\sim$7% artificial FRD into our measurements.

$$F/\#_{out} = \frac{F/\#_{in}}{(1 + 2\theta F/\#_{in})} \tag{1}$$

To improve upon this alignment the following method was adopted. Small, precise, tips and tilts are made to the input IFU head and images of the output spots taken. By then plotting the EE as a function of radius for each tip or tilt, a minimum in the FRD profile is located. These deviations can clearly be seen in the left-hand plot in figure 6 (dotted lines). As each tip or tilt introduces a $\sim$0.002 radian deviation from the current alignment, iterations with this technique lead to a FRD minimum having 1.5% artificial FRD. This method proves extremely repeatable and effective in minimizing slight misalignments of the input beam and the fiber axis.

There is an aspect of figure 6 that warrants consideration. Note the cross over of the heavy line (deemed the best alignment) to the dotted lines seen in the left-hand plot of figure 6. This is to be expected; FRD scatters light not only outwards, but into the central obscuration and gives rise to this characteristic cross over. The same cross over is also seen in both plots of figure 9. This is significant as the spread in our wavelength dependent tests (figure 8) do not exhibit this characteristic cross-over. It is this lack of cross over, in part, that leads us to conclude FRD is wavelength *independent* down to 365 nm.[‖] A second test was conducted, confirming this result, the details of which are given in section 5.

Coupling efficiency is critical for accurate transmission measurements. This is particularly important for our measurement method, which relies on visually coupling the input spot into the fiber. To address this concern,

[‖] We conducted FRD tests at 337 nm, yet due to the slight red leak in this filter the results fell near those taken at 400 nm. Although the 337 nm data is not presented it also showed no evidence for any FRD wavelength dependence, once the red leak was taken into account.

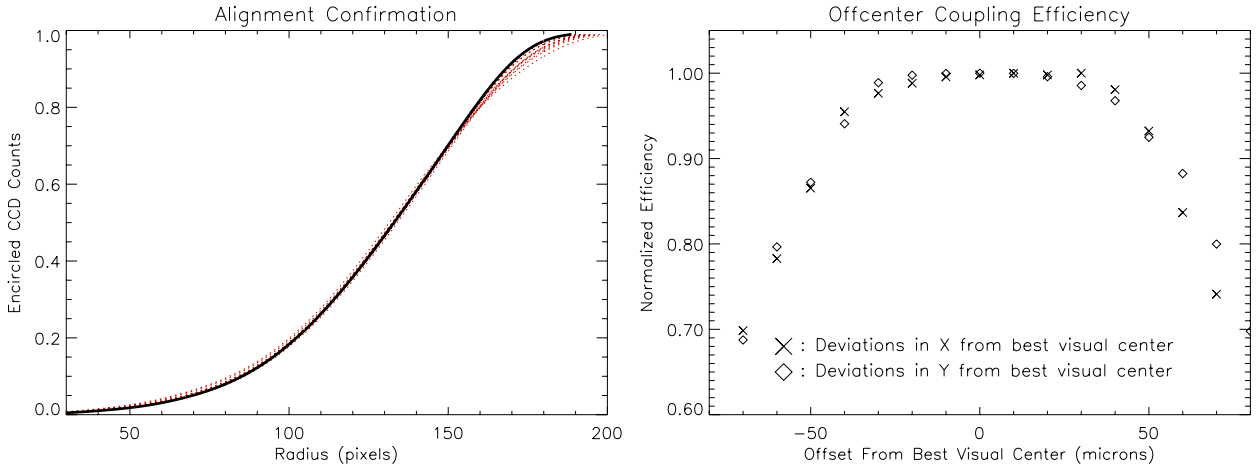

Figure 6. The left figure plots relative intensity as a function of radial position and is used to confirm the degree of orthogonality of the input spot to the fiber axis. This technique achieves alignment to within ±0.002 radians and was extremely repeatable over several iterations. The details of this method are given in the text. The second figure reflects the accuracy achieved by visually centering the input spot onto the fiber.

we've explored how far from best visual center our input spot can be before we begin to loose coupling efficiency. The right-hand plot in figure 6 shows our coupling efficiency remains near 100% up to ±30 μm from best visual center. At >30 μm we see a drop in coupling efficiency of 3-5%. As the repeatability of our measurements on the same fiber is consistently better than 2%, we are confident the systematic errors due to our method of coupling is minimal.

4. TESTING METHOD

Both our transmission and focal ratio degradation measurements make use of an APOGEE U-260 (512x512 20 μm/pixel) liquid-cooled CCD camera. Both techniques described here are simple in concept and analysis, requiring only a precision translation stage, a CCD camera and a method for coupling light of a known f-ratio into a fiber. The data is collected as FITS files with MAXIM-DL, and all data reduction and analysis is completed with IDL routines written for the various tasks.

4.1 A Differential Method for Testing FRD

There are a variety of methods to test FRD in optical fibers. The method we use is a variation on the relatively simple geometric analysis of the output spot size when the separation between the output end of the fiber and the CCD are known. The primary drawback of this method is that it requires precise knowledge of the distance between the end of the fiber and the CCD. This becomes an overwhelming challenge when attempting to make measurements on large numbers of fibers, or when the fiber-to-CCD separation can not be accurately determined. To avoid this difficulty, we make use of a simple, differential method that does not require any knowledge of the separation between the CCD and the output end of the fiber. The technique is described below.

The measurement of the f-ratio of a beam (either input or output) is made by stepping the CCD camera in well-defined increments, in our case 1.27 mm (0.05"), and imaging the far field of the output spot. Then, by comparing the same encircled energy radius at two camera positions, an estimate of the output f-ratio is made. Each set of camera positions gives you an estimate of the f-ratio of the beam by taking the ratio of the camera translation distance to the change in spot size diameter of equal EE values. Indeed, after the first two spot images are taken, yielding one measurement, additional camera positions increase your total number of measurements by n-1, where 'n' is the number of camera positions for a given fiber. This is accomplished by comparing step 1 to step 3, step 1 to step 4, and so on. Repeat FRD measurements on the same fibers show this method to return very consistent results (to within 2%) even when the measurements are separated by several weeks.

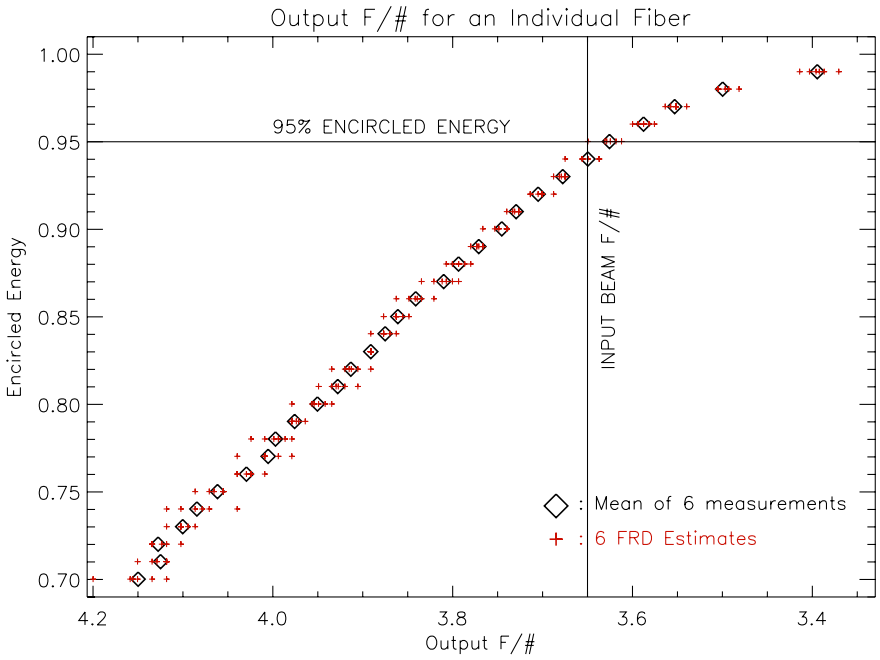

Figure 7. A plot showing a typical FRD measurement at 600 nm at our input beam of F/3.65 for a Polymicro fiber in the VP2 IFU. The '+'s mark the 6 measurements yielded from the differential step measurement method described in section 4.1. This scatter is typical for the measurements at all wavelengths. The black diamonds are the mean of the 6 values, after a minmax rejection of 1. These measurements were taken with both cover plates and index-matching gel.

4.2 The Transmission Testing Method

The transmission measurements presented in section 6 are made by taking the ratio of the total light exiting a fiber at a given wavelength to the total light entering the fiber. To accomplish this, the IFU head translation stage is mounted on a sliding stage allowing the entire assembly to move out of the optical path of the test bench. The CCD camera is then set just beyond focus, and a 200 μm pinhole is set at focus to block any stray light that would not make it into the 200 μm fiber. A set of five frames at each wavelength (referred to as *baseline* images) are taken in the far field, after the last baffling pinhole. Background frames are taken by blocking the light at the *entrance* pinhole. After a set of 50 baseline frames is taken (5x 10 filters) the camera is repositioned to the output end of the fiber bundle and the IFU head is translated back to the focus of the optical bench. A set of 2 to 3 fibers are then tested at all 10 wavelengths, followed by another set of baseline frames. This entire process takes approximately 1.5 hours.

The accuracy of this method relies, in part, on the stability of the light source over this time period. Tests of the light source show it to be stable to rapid fluctuations (on time scales of seconds to minutes) to below 1%. However, we do find the source to have a gradual drift in intensity over a time period of $\sim$6 hours with an amplitude of $\sim$7%. This is a sinusoidal fluctuation which is nearly linear over the time duration between baseline exposures. We make a simple correction for this effect by linearly interpolating, in time, between the two neighboring baseline frames and the data frame. This allows us to determine the best baseline value to use in our estimate of absolute transmission. As the quantum efficiency of our CCD is much lower in the UV, a wide range of integration times are required, ranging from 0.3 seconds at 600 nm to 60 seconds at 337 nm. After the background frames are subtracted from the data, the total counts on the chip are summed. As our test bench is light tight and our background subtraction is excellent, including the entire chip in the sum makes no discernible difference in the totals. As the spot size takes up roughly half of the chip, flat-fielding is not required. This technique has proven robust; repeated measurements on the same fibers, often separated by months, returns transmission values to within $\pm$1.5% at all wavelengths.

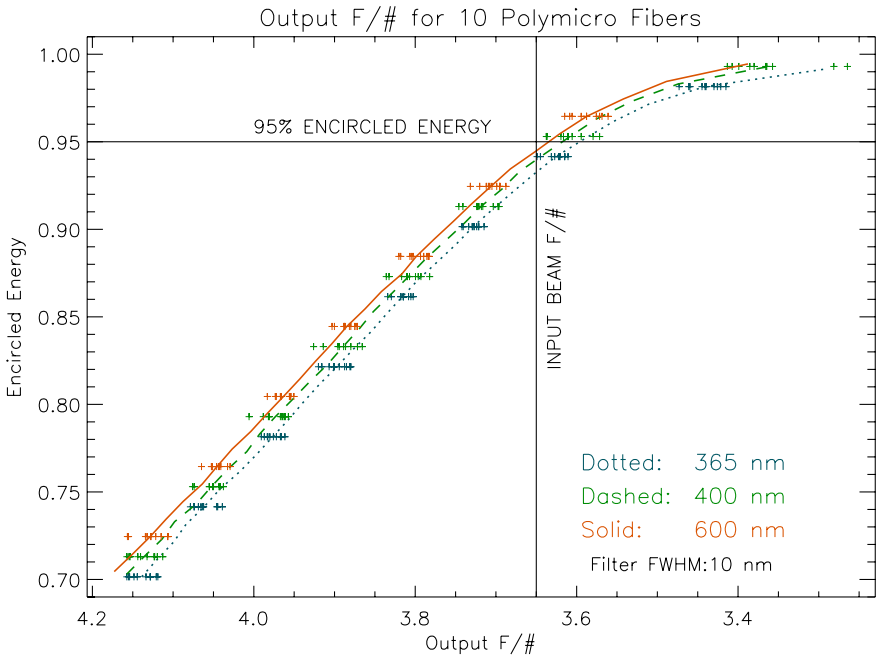

Figure 8. A plot exploring the wavelength dependence of the 4 fiber types tested. The '+'s denote the mean value of the 10 Polymicro fibers tested in VP2 (i.e. the diamonds in figure 7). We've suppressed the majority of the data for visual clarity. Although there appears to be a wavelength dependence, this is most likely a systematic effect due to scattering off the the pickoff mirrors rather than FRD, as discussed in the text.

5. THE FOCAL RATIO DEGRADATION MEASUREMENTS

Figure 7 shows the results of a typical FRD measurement of one Polymicro fiber at 600 nm. As our input f-ratio is fixed at F/3.65 for these tests we plot EE as a function of output f-ratio for all the FRD plots shown. For reference, a vertical line at F/3.65 and a horizontal line denoting 95% EE are plotted. The diamonds in figure 7 plot the mean, after a minmax rejection of 1 point, of the 6 measurements (shown as +'s). At 95% EE the output f-ratio for this fiber is F/3.63, corresponding to an FRD value of 1.008.

In all, 24 fibers in VP2 were tested for FRD both before and after installation of the AR cover plates and index matching gel. Although no figure is presented here, we found a 5-7% improvement in FRD with the AR cover plates over measurements made on the same fibers without the cover plates. This improvement in FRD with installation of the cover plates was uniform across both wavelength and fiber type. Of the 24 fibers tested in VP2, 10 of these were Polymicro FBP200/200/245 NA:0.22 fibers, the same type of fiber used in VP1. Plotted in figure 8 is the mean output f-ratios for all 10 Polymicro fibers in VP2. Here, the '+'s denote measurements of the *mean value* of each of the ten fibers (i.e. the diamonds in figure 7).

Figure 8 summarizes the most significant finding of this work. Namely, we find no evidence for an FRD wavelength dependence down to 365 nm (see footnote in section 3.1). Although a first glance at figure 8 appears to show a wavelength dependence on FRD, we believe this is a systematic effect, possibly due to wavelength dependent scattering off the test bench pickoff mirrors. The evidence for a lack of wavelength dependence on FRD is two-fold. As first discussed in section 3.1, the comparison plots of FRD should exhibit a cross over, as FRD scatters light both outwards and into the central obscuration. This is not seen in figure 8, even when we consider lower EE values not shown in the plot. To confirm this result, a second series of FRD tests were conducted at a slower input beam than F/3.65. If caused by FRD the separation between the three lines in figure 8 should increase, as FRD in known to increase with slower input beams. We conducted FRD tests at an input beam of ∼F/6 and saw no increase in the separation at all wavelengths tested. These two pieces of evidence lead us to conclude that if there is a wavelength dependence on FRD it is an extremely weak one.

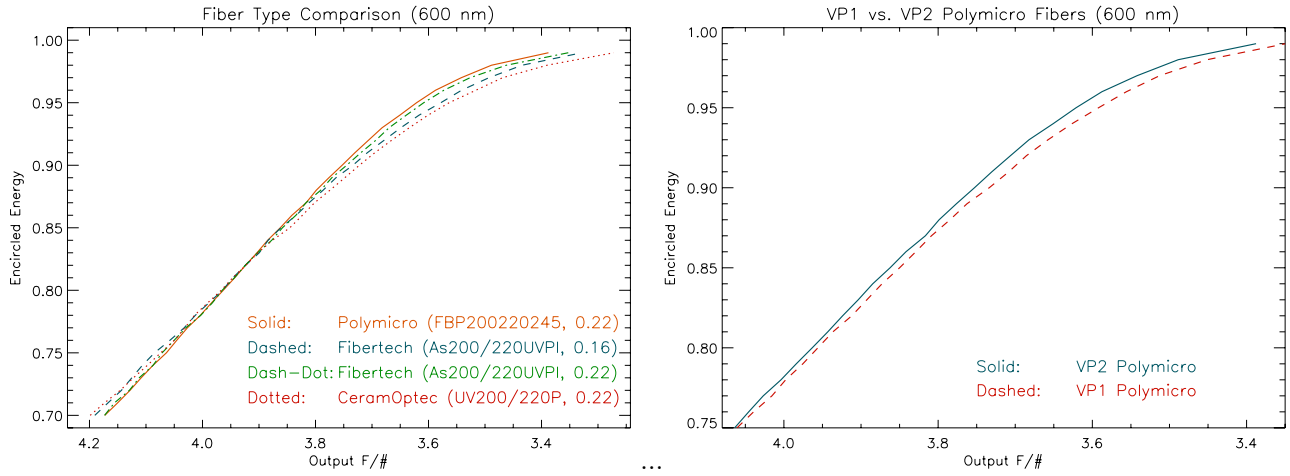

Figure 9. The figure on the left shows the difference in FRD for 4 fiber types at 600 nm. Although only one wavelength is plotted here, similar results were seen at 400 nm and 365 nm. On the right is shown a comparison of VP1 and the Polymicro fibers in VP2 at 600 nm. Although VP2 is 3 times the length of VP1 it exhibits less FRD than VP1. This is likely due to the difference in mounting and end polish between the two IFUs as discussed in section 2.1. Note that the range of the ordinate has been slightly altered.

The same reduction and analysis was made on the other three types of fibers in VP2 and on the shorter Polymicro fibers in VP1. The left plot in figure 9 shows the results for all four fiber types in VP2. As in figure 8 we have plotted the mean of all the fibers tested, separated by fiber type. The solid line (orange in the electronic version) in both figure 8 and the left plot of figure 9 are identical. As the spread in the results was very similar at all wavelengths tested for all fibers, we present only the plot for 600 nm. The Polymicro fibers proved superior to the other 3 types of fibers tested, with CeramOptec exhibiting the worst performance. However, despite the differences seen in these fiber types, all 4 are well within the specification of achieving 95% EE within an F/3.36 output beam.

The right plot in figure 9 compares the results of the Polymicro fibers in both VP1 (4.5 m) and VP2 (15 m) at 600 nm. Interestingly, VP2 shows less FRD at all three wavelengths than VP1. If FRD exhibits a length dependence, it is obscured at these lengths by the effects of end polish and mounting technique.

6. THE TRANSMISSION MEASUREMENTS

Both VP1 and VP2 have AR cover plates installed at both the input and output ends of the fiber bundle.[16] In the case of VP2, we were able to conduct transmission measurements both before and after installation of the cover plates. Nineteen fibers were tested before installation of the cover plates and 24 after installation. There are a number of significant outcomes of these tests. First, the overall transmission before installation of the AR cover plates is below the theoretical values for the Polymicro FBP200/220/245 fibers by ∼4-6% at all wavelengths. This is certainly due to end loss reflections. Despite this offset, the overall shape of the transmission curve matches the theoretical values quite well. The left plot in figure 10 shows all of the fibers tested before installation of the cover plates while the the right plot shows the mean values for each of the four fiber types.** Notable in this result is the superior performance of the Polymicro fibers at all wavelengths, particularly at 600 nm. Also of note is the unexpected rise at 337 nm- this is not real, but the result of a red leak in this filter.

After installation of the two AR cover plates we see the expected improvement over most of the wavelengths. However, we find that transmission is significantly down, beginning at 380 nm and decreasing by ∼10% at 337 nm. This drop in the UV transmission is due to the index-matching gel (Dow Corning Q2-3067). We are exploring alternatives to this gel as this substantial loss in the UV is unacceptable.

**The lowest fiber in figure 10 was not included in the calculation of the mean transmission value. This fiber had a fracture in its output end. Replotted in figure 11 ('*' symbols), note the significant improvement in overall transmission caused by the index-matching gel.

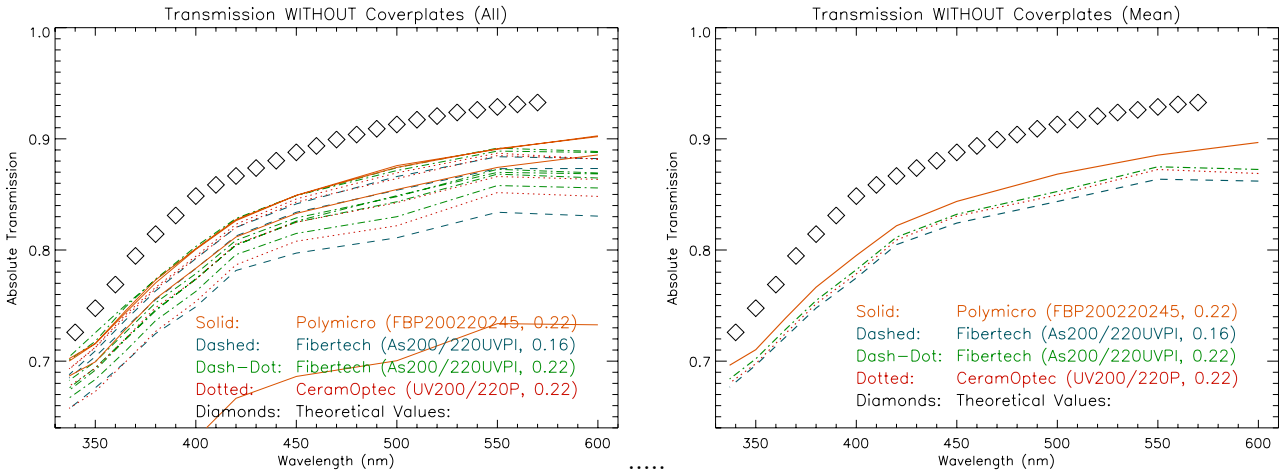

Figure 10. The left-hand plot shows data for all fibers tested for transmission *before* installation of the AR cover plates and index-matching gel. The plot on the right shows the mean for each of the four fiber types. The rise in transmission at 337 nm is due to a red leak in that filter.

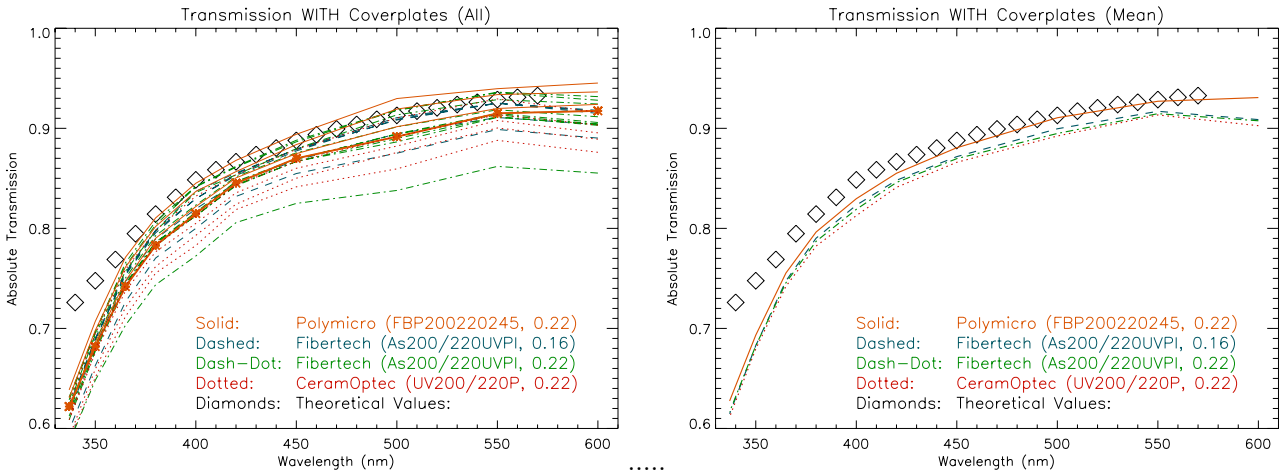

Figure 11. The left-hand plot shows data for all fibers tested for transmission *after* installation of the AR cover plates and index-matching gel. The plot on the right shows the mean for each of the four fiber types. Comparing these plots to figure 10, the strong absorption of the index-matching gel is clear. Also note the significant improvement seen in the fractured fiber, denoted with a heavier line and stars. This shows the clear benefits of end immersion.

7. CONCLUSIONS

We have presented the details of a new fiber optic test bench constructed at the University of Texas, Austin, in order to conduct FRD and transmission measurements on two prototype IFUs for the VIRUS-P integral field spectrograph. Also included is a detailed description of a simple differential method of testing FRD, and a method for ensuring orthogonal coupling into fibers to within ±0.1 degrees.

All fibers tested performed well within the specifications of the instrument design. For all fibers tested the average FRD (EE: 95%) over the wavelength range of 365 nm to 600 nm is 1.02. There was no apparent wavelength dependence on FRD over this range.

The author would like to thank Stuart Barnes and Joshua Adams for many helpful discussions in both the development of the test bench and analysis of the results.

REFERENCES

[1] Haynes, R., Lee, D., Allington-Smith, J., Content, R., Dodsworth, G., Lewis, I., Sharples, R., Turner, J., Webster, J., Done, C., Peletier, R., Parry, I., and Chapman, S., "Multiple-Object and Integral Field Near-Infrared Spectroscopy Using Fibers," **111**, 1451–1468 (Nov. 1999).

[2] Haynes, R., Bland-Hawthorn, J., Large, M. C., Klein, K.-F., and Nelson, G. W., "New age fibers: the children of the photonic revolution," in [*Optical Fabrication, Metrology, and Material Advancements for Telescopes, Edited by E. Atad-Ettedgui and P. Dierickx. Proceedings of the SPIE, Volume 5494, pp. 586-597 (2004).*], Atad-Ettedgui, E. and Dierickx, P., eds., *Presented at the Society of Photo-Optical Instrumentation Engineers (SPIE) Conference* **5494**, 586–597 (Sept. 2004).

[3] Parry, I. R., "Optical fibres for integral field spectroscopy," *New Astronomy Review* **50**, 301–304 (June 2006).

[4] Avila, G., "Tests of optical fibres for astronomical instrumentation at ESO," in [*Fiber Optics in Astronomy*], Barden, S. C., ed., *Astronomical Society of the Pacific Conference Series* **3**, 63–73 (1988).

[5] Craig, W. W., Hailey, C. J., and Brodie, J. P., "Measurement of fibers to be used in fiber fed spectroscopy," in [*Fiber Optics in Astronomy*], Barden, S. C., ed., *Astronomical Society of the Pacific Conference Series* **3**, 41–51 (1988).

[6] Avila, G., "Results on Fiber Characterization at ESO," in [*Fiber Optics in Astronomy III*], Arribas, S., Mediavilla, E., and Watson, F., eds., *Astronomical Society of the Pacific Conference Series* **152**, 44–+ (1998).

[7] Ramsey, L. W., "Focal ratio degradation in optical fibers of astronomical interest," in [*Fiber Optics in Astronomy*], Barden, S. C., ed., *Astronomical Society of the Pacific Conference Series* **3**, 26–39 (1988).

[8] Clayton, C. A., "The implications of image scrambling and focal ratio degradation in fibre optics on the design of astronomical instrumentation," **213**, 502–515 (Apr. 1989).

[9] Carrasco, E. and Parry, I. R., "A method for determining the focal ratio degradation of optical fibres for astronomy," **271**, 1–+ (Nov. 1994).

[10] Schmoll, J., Roth, M. M., and Laux, U., "Statistical Test of Optical Fibers for Use in PMAS, the Potsdam Multi-Aperture Spectrophotometer," **115**, 854–868 (July 2003).

[11] Bershady, M. A., Andersen, D. R., Harker, J., Ramsey, L. W., and Verheijen, M. A. W., "SparsePak: A Formatted Fiber Field Unit for the WIYN Telescope Bench Spectrograph. I. Design, Construction, and Calibration," **116**, 565–590 (June 2004).

[12] MacQueen, P. J., Hill, G. J., Smith, M. P., Tufts, J. R., Barnes, S. I., Roth, M. M., Kelz, A., Adams, J. J., Blanc, G., Murphy, J. D., Altmann, W., Wesley, G. L., Segura, P. R., Good, J. M., Goertz, J. A., Edmonston, R. D., and Wilkinson, C. P., "Design, construction, and performance of VIRUS-P: the prototype of a highly replicated integral field spectrograph for the HET," in [*Astronomical Telescopes and Instrumentation*], *Proc. SPIE* **7014-257** (2008).

[13] Hill, G. J., Gebhardt, K., Komatsu, E., Drory, N., MacQueen, P. J., Adams, J. J., Blanc, G. A., Koehler, R., Rafal, M., Roth, M. M., Kelz, A., Gronwall, C., Ciardullo, R., and Schneider, D. P., "The Hobby-Eberly Telescope Dark Energy Experiment (HETDEX): Description and Early Pilot Survey Results," in [*Panoramic Views of the Universe*], *ASP conference series* (2008).

[14] Roth, M. M., "The AIP Photometric Testbench," in [*Optical Detectors for Astronomy*], Beletic, J. and Amico, P., eds., *Astrophysics and Space Science Library* **228**, 153–+ (1998).

[15] Grupp, F., "Measuring the properties of optical fibers: First results from the AIP fiber testbench for fiber bundle IFUs," *New Astronomy Review* **50**, 323–325 (June 2006).

[16] Kelz, A., Bauer, S. M., Grupp, F., Hill, G. J., Popow, E., Palunas, P., Roth, M. M., MacQueen, P. J., and Tripphahn, U., "Prototype development of the integral-field unit for VIRUS," in [*Optomechanical Technologies for Astronomy. Edited by Atad-Ettedgui, Eli; Antebi, Joseph; Lemke, Dietrich. Proceedings of the SPIE, Volume 6273, pp. 62733W (2006).*], *Presented at the Society of Photo-Optical Instrumentation Engineers (SPIE) Conference* **6273** (July 2006).